

UC Davis

UC Davis Previously Published Works

Title

Structural proof of a [C-F-C]⁺ fluoronium cation.

Permalink

<https://escholarship.org/uc/item/8hj3v0br>

Journal

Nature Communications, 12(1)

Authors

Hoffmann, Kurt

Wiesner, Anja

Müller, Carsten

et al.

Publication Date






2021-09-06

DOI


10.1038/s41467-021-25592-6

Peer reviewed

Structural proof of a $[\text{C-F-C}]^+$ fluoronium cation

Kurt F. Hoffmann¹, Anja Wiesner¹, Carsten Müller¹, Simon Steinhauer ¹, Helmut Beckers¹,
Muhammad Kazim ², Cody Ross Pitts^{2,3}, Thomas Lectka²  & Sebastian Riedel ¹ 

Organic fluoronium ions can be described as positively charged molecules in which the most electronegative and least polarizable element fluorine engages in two partially covalent bonding interactions to two carbon centers. While recent solvolysis experiments and NMR spectroscopic studies on a metastable $[\text{C-F-C}]^+$ fluoronium ion strongly support the divalent fluoronium structure over the alternative rapidly equilibrating classical carbocation, the model system has, to date, eluded crystallographic analysis to confirm this phenomenon in the solid state. Herein, we report the single crystal structure of a symmetrical $[\text{C-F-C}]^+$ fluoronium cation. Besides its synthesis and crystallographic characterization as the $[\text{Sb}_2\text{F}_{11}]^-$ salt, vibrational spectra are discussed and a detailed analysis concerning the nature of the bonding situation in this fluoronium ion and its heavier halonium homologues is performed, which provides detailed insights on this molecular structure.

¹Fachbereich Biologie, Chemie, Pharmazie, Institut für Chemie und Biochemie – Anorganische Chemie, Freie Universität Berlin, Berlin, Germany. ²Department of Chemistry, Johns Hopkins University, Baltimore, MD, USA. ³Present address: Department of Chemistry, University of California, Davis, Davis, CA, USA.
email: lectka@jhu.edu; s.riedel@fu-berlin.de

According to IUPAC, halonium ions are defined as ions of the form $[R_2X]^+$, where X may be any halogen¹. In the case of organic halonium ions, R is defined as a cyclic or open-chained hydrocarbon backbone. Since they were first discussed as reactive intermediates in organic halogenation reactions in 1937², a large variety of stable and structurally characterizable iodo^{3,4}, bromo^{5,6}, and chloronium^{7–9} salts of the type $[C-X-C]^+$ have been synthesized^{10,11}. On the other hand, fluoronium cations, in which a divalent fluorine atom (as depicted in a simplifying Lewis dot structure) is symmetrically bound to two carbon atoms, have only been reported thus far in spectroscopic investigations. For instance, Morton et al. first detected a three-membered cyclic fluoriranium ion as an intermediate in mass-spectrometry experiments¹², while Gabbaï and coworkers obtained the structure of a diphenylnaphthylmethylium cation that shows an intramolecular bonding interaction to an adjacent fluorine substituent, allowing a description as an unsymmetrically bridged fluoronium cation (Fig. 1a)¹³.

In 2013, Lectka et al. presented the transient generation of a symmetrically bridged fluoronium cation in solution starting from a rigid double-norbornyl type precursor. Its formation as a fleeting reactive intermediate was indicated through isotopic labeling experiments^{14,15}. Finally, in 2018 they supported the formation of the aforementioned fluoronium ion by NMR spectroscopy^{16,17}; yet, the structural proof of this organic fluoronium ion in the solid state remained a lofty goal. In addition to these few spectroscopic examples of carbon-based fluoronium cations, some inorganic fluoronium cations have been investigated in the past. Motz and Bartmann published in 1988 a crystal structure of the simplest fluoronium ion $[H_2F]^+$ ¹⁸. A crystal structure of a cyclic disilylfluoronium salt was reported by Müller and coworkers in 2006, followed by the structure of an open-chained bisilylated fluoronium cation by Schulz in 2009^{19–21}. More recently in 2018, Kraus presented examples of a fluorine atom coordinated by two BrF_2 units (Fig. 1a)^{22,23}.

In this work, we present a modified synthesis and structural investigation of the carbon-based double-norbornyl type fluoronium

ion **1** (Fig. 1) as the $[Sb_2F_{11}]^-$ salt by single-crystal X-ray diffraction. Furthermore, the bonding schemes of $[C-X-C]^+$ ($X = F, Cl, Br, I$) are discussed and compared through detailed AIM analyses, and the properties of **1** are further analyzed by vibrational spectroscopy.

Results

Synthesis and characterization. Our approach is, in principle, based on utilizing the strong Lewis acid SbF_5 as a fluoride ion abstractor^{16,17}. Herein, neat SbF_5 was substituted by the crystalline solvent-adduct $SbF_5 \cdot SO_2$ due to its slightly weakened acidic character and more convenient handling (Fig. 1b). By adding precursor **2** to a cooled mixture of $SbF_5 \cdot SO_2$ in SO_2ClF , a yellow solution is formed. Partial evaporation of the SO_2ClF and consecutive slow cooling of the reaction mixture afforded single crystals suitable for X-ray diffraction.

The compound $[1][Sb_2F_{11}] \cdot (SO_2ClF)_3$ (Fig. 2, more detailed structure in Supplementary Fig. 1 including a comprehensive list of crystal data in Supplementary Tables 1–3) crystallizes in the centrosymmetric monoclinic space group $P2_1/c$ along with three solvent molecules per asymmetric unit. A nearly symmetrical C–F–C bonding array is observed. The bridging fluorine atom F1 and its adjacent carbon atoms feature bond lengths of 156.6(3) and 158.5(3) pm with an overall C1–F1–C2 bond angle of 115.78(15)°. This is consistent with the data of the computed quantum-chemical structure of cation **1** with C–F bond distances of 157.4 and 160.1 pm and a C–F–C angle of 115.32° (B3LYP/cc-pVTZ). Compared to the unsymmetrical bridging fluorine atom in Gabbaï's bis-naphthalene complex with C–F distances of 142.4 and 244.4 pm, the distances in cation **1** are in between¹³. No interaction between anion and cation can be observed, although as predicted in previous publications, a single SbF_5 coordinates to the anhydride function of the cation. The coordinating SbF_5 is slightly bent out of the anhydride plane with a dihedral angle $\angle(O2-C14-O1-Sb1) = 19.0(4)^\circ$, resulting in a C_1 symmetry of the cation. Lectka et al. previously assumed C_s symmetry from their NMR analysis of this compound^{16,17}.

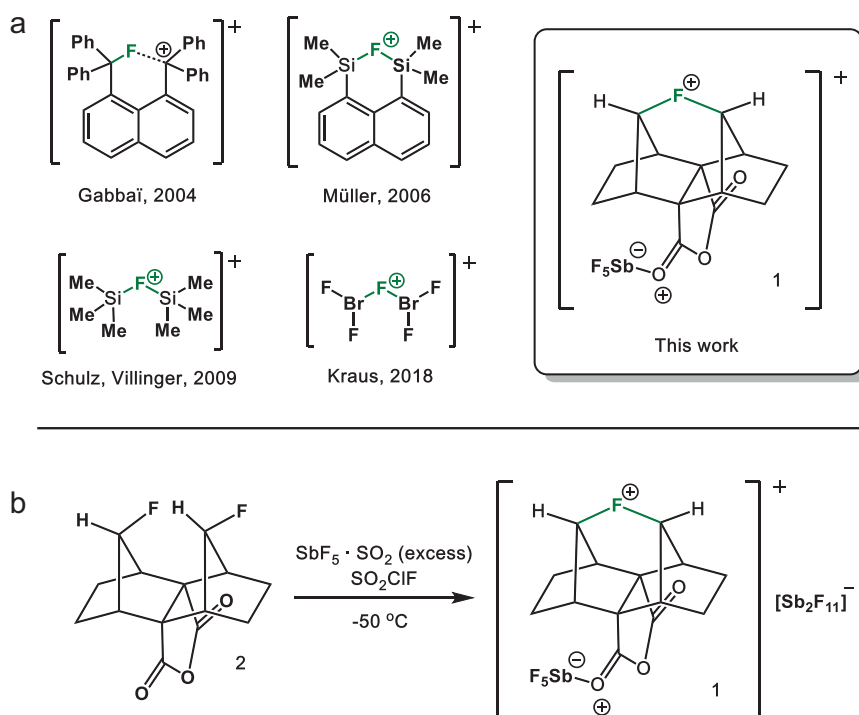


Fig. 1 Overview of fluoronium ions in the condensed phase. **a** Crystallographically characterized fluoronium ions^{16,17,19–23}. Note that the formal charges shown inside a circle do not represent the actual charge of the corresponding atoms. **b** Synthesis of the fluoronium salt $[1][Sb_2F_{11}]$.

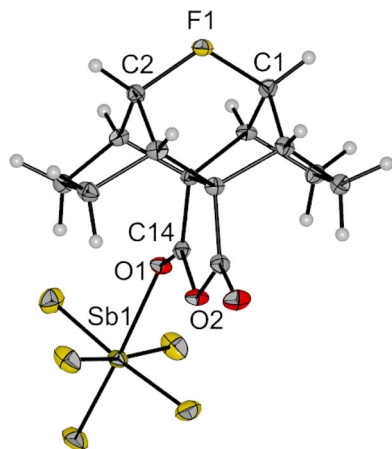


Fig. 2 Molecular structure of the fluoronium ion **1** as its $[\text{Sb}_2\text{F}_{11}]^-$ (SO_2ClF)₃ salt in the solid state. Anion and solvent molecules are not depicted. Thermal ellipsoids set to 50% probability. Selected bond lengths [pm] and angles [°]: F1-C1 156.6(3), F1-C2 158.7(3), C1-F1-C2 115.64(17), O2-C14-O1-Sb1 19.0(4).

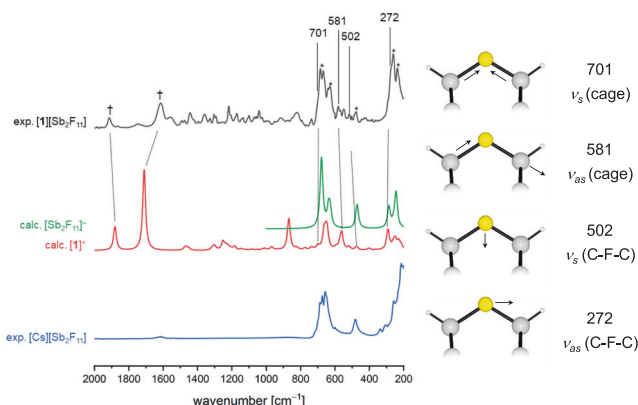


Fig. 3 Vibrational analysis of fluoronium **1**. Left: Experimental infrared spectra of $[\mathbf{1}][\text{Sb}_2\text{F}_{11}]$ (black) and $[\text{Cs}][\text{Sb}_2\text{F}_{11}]$ (blue) at -40°C , as well as calculated spectra of cation **1** (red) and anion $[\text{Sb}_2\text{F}_{11}]^-$ (green) at B3LYP/def2-TZVP level of theory. Bands of the anion are denoted with an asterisk in the experimental spectrum and bands associated with the carbonyl group are denoted with a dagger. Right: Approximate representation and assignment of selected C-F-C normal modes of **1** (see text, only displacements involving the C-F-C unit are shown).

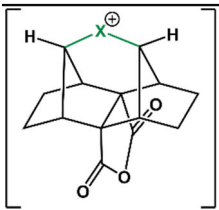
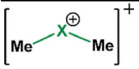
The vacuum-dried crystalline material was investigated by IR spectroscopy at -40°C . The experimental spectrum of $[\mathbf{1}][\text{Sb}_2\text{F}_{11}]$ (see Fig. 3, black trace) was assigned guided by calculated vibrational spectra of cation **1** and anion $[\text{Sb}_2\text{F}_{11}]^-$ and by comparison with the spectrum of precursor **2** (Supplementary Fig. 3 and Supplementary Table 5), and an experimental spectrum of $[\text{Cs}][\text{Sb}_2\text{F}_{11}]$. This allows the assignment of characteristic vibrational modes at 581 cm^{-1} (calc. 560 cm^{-1}) and 502 cm^{-1} (calc. 471 cm^{-1}) carrying significant in-plane C-F-C stretching character. Although the region around 690 cm^{-1} and 260 cm^{-1} are dominated by strong Sb_2F_{11} vibrations two additionally fluorine-involved modes are tentatively assigned to shoulders at 272 cm^{-1} (calc. 291 cm^{-1}) and 701 cm^{-1} (calc. 699 cm^{-1}). In addition, the coordination of SbF_5 to one of the carbonyl groups of **1** leads to a splitting of the C=O bands at $1913\text{ (}\nu(\text{C}=\text{O}))$ and $1614\text{ (}\nu(\text{C}=\text{O}\cdots\text{SbF}_5))\text{ cm}^{-1}$ (marked by a dagger symbol in Fig. 3). For a complete list of recorded IR vibrations and their assignment see also the methods section.

In Table 1 we present a comparison of the C-F-C stretching modes for the acyclic dimethyl halonium ions $[\text{Me}_2\text{X}]^+$ ($\text{X} = \text{F}, \text{Cl}, \text{Br}$ and I) with those of the C_{2v} symmetric double-norbornyl halonium ions $[\text{DN}(\text{TX})]^+$ (without coordination of an additional SbF_5 group). Generally, such a comparison is hampered by the more complex and rigid cage shape of the $[\text{DN}(\text{TX})]^+$ derivatives, since the division of such cage vibrations into certain stretching and ring deformations is more arbitrary and the vibrational coupling between different cage vibrations is more serious than for the simple dimethyl analogs. In Fig. 3 and Table 1 we present a tentative assignment of characteristic vibrations of **1** and the symmetric $[\text{DN}(\text{TX})]^+$ ions, respectively. A closer look reveals that the C-X-C stretching coordinates of the $[\text{DN}(\text{TX})]^+$ ions contribute to several normal modes such as an in-phase and an out-of-phase cage vibration, denoted as $\nu_s(\text{cage})$ and $\nu_{as}(\text{cage})$ in Table 1 and Fig. 3, respectively, in which mainly the two carbon atoms vibrate along the C-X coordinates, as well as to two lower-lying modes which carry dominant halogen atom displacements, and which are thus denoted as $\nu_s(\text{C-X-C})$ and $\nu_{as}(\text{C-X-C})$ stretching vibrations (for more details see Supplementary Movie 1). As a consequence, the $\nu_s(\text{cage})$ frequencies change only slightly from $\nu_s = 724\text{ cm}^{-1}$ ($[\text{DN}(\text{TF})]^+$) to 709 cm^{-1} ($[\text{DN}(\text{TI})]^+$), while the $\nu_s(\text{C-X-C})$ stretching frequencies in the $[\text{DN}(\text{TX})]^+$ ions are strongly reduced from $\nu_s = 488\text{ cm}^{-1}$ for $\text{X} = \text{F}$ down to 365 cm^{-1} for $\text{X} = \text{I}$ (Table 1).

The C-F-C stretching vibrations of **1** and the symmetric $[\text{DN}(\text{TF})]^+$ cation are strongly red-shifted compared to conventional monovalent C-F vibrations (usually observed between 1300 and 900 cm^{-1})²⁴, indicating the weakened C-F bonds in these fluoronium derivatives. This is in line with similar findings of Dopfer et al. and their calculations on phenylfluoronium $[\text{F-C}_6\text{H}_5\text{F}]^+$ ²⁵. Also, the significantly higher frequency of the symmetric compared to the antisymmetric C-F-C stretching modes for the $[\text{DN}(\text{TX})]^+$ cations is remarkable and in striking contrast to spectroscopic investigations of acyclic dialkyl halonium salts^{26,27}.

In addition, the comparison of the frequencies of the cyclic $[\text{DN}(\text{TX})]^+$ ions with those of the $[\text{Me}_2\text{X}]^+$ derivatives reveals further interesting features: while the $\nu_{as}(\text{C-X-C})$ vibrations of the $[\text{DN}(\text{TX})]^+$ ions generally occur at lower frequencies than those of the $[\text{Me}_2\text{X}]^+$ analogs, the two antisymmetric vibrations of $[\text{DN}(\text{TF})]^+$ are even lower in frequency than those of $[\text{DN}(\text{Cl})]^+$ (Table 1). We tentatively attribute these characteristic spectroscopic properties to different bonding properties of the C-X-C bonds in $[\text{DN}(\text{TF})]^+$ and $[\text{Me}_2\text{F}]^+$ on the one hand and the $[\text{DN}(\text{Cl})]^+$ cation on the other. A distortion along the antisymmetric stretching coordinate is expected to change the overall wave-function by increasing the relative weight of a carbo-cationic resonance structure with unequal C-F-C bond distances, and, consequently, the stabilization of this carbo-cationic resonance structure by suitable carbon substituents in a fluoronium equilibrium structure should result in a lower antisymmetric stretching frequency. This assumption was previously supported by an almost linear decrease in $\nu_{as}(\text{C-Cl-C})$ on the number of methyl groups n in the acyclic chloronium cations $[(\text{H}_3\text{C})_n(\text{H}_{3-n}\text{C})_2\text{Cl}]^+$ ($n = 0-3$)²⁷. Thus, lower $\nu_{as}(\text{C-X-C})$ frequencies are to be expected for the $[\text{DN}(\text{TX})]^+$ cations with secondary carbon substituents compared to the $[\text{Me}_2\text{X}]^+$ series. Also, entropic effects likely contribute to the stabilization of the cyclic $[\text{DN}(\text{TX})]^+$ cations. In addition, we have carried out a vibrational analysis of $[\text{DN}(\text{TX})]^+$ cations, with $\text{X} = \text{F}$ and Cl , in which the hydrogen atoms of the H-C groups next to X are substituted by $\text{R} = \text{F}, \text{CH}_3$, and CF_3 (denoted as $[\text{R}_2\text{DN}(\text{TX})]^+$ in Supplementary Table 4). With the exception of the fluorinated derivative $[\text{F}_2\text{DN}(\text{TF})]^+$ ($\text{R} = \text{F}$) all other computed derivatives form stable symmetric halonium cations and for $[\text{F}_2\text{DN}(\text{TF})]^+$, we have

Table 1 Comparison of selected computed vibrational frequencies and C–X–C bond angles of dimethyl halonium ions [Me₂X]⁺ (X = F, Cl, Br, I) and double-norbornyl type halonium ions [DNTX]⁺ (C_{2v} symmetry) at def2-TZVPP/B3LYP level of theory.

	ν_s (cage)	ν_s (C–X–C)	ν_{as} (cage)	ν_{as} (C–X–C)	\angle (C–X–C)	
	[DNTF] ⁺	724 (6)	488 (6)	588 (29)	304 (34)	115°
	[DNTCl] ⁺	711 (11)	386 (4)	657 (22)	313 (3)	98°
	[DNTBr] ⁺	710 (15)	368 (4)	651 (19)	253 (2)	92°
	[DNTI] ⁺	709 (18)	365 (3)	649 (14)	234 (1)	86°
	ν_s (C–X–C)	δ (C–X–C)	ν_{as} (C–X–C)	\angle (C–X–C)		
	[Me ₂ F] ⁺	659 (12)	264 (1)	677 (100)	121°	
	[Me ₂ Cl] ⁺	561 (41)	228 (1)	604 (100)	105°	
	[Me ₂ Br] ⁺	500 (55)	187 (4)	517 (100)	101°	
	[Me ₂ I] ⁺	470 (41)	160 (3)	484 (52)	98°	

Frequencies are given in cm⁻¹. Relative intensities are given in brackets.

analyzed the C_{2v} symmetric fluoronium transition state, connecting two equivalent carbo-cationic minimum structures (Supplementary Fig. 2). For R = CH₃ and F, which both support an asymmetric carbo-cationic structure the fluoronium ions (X = F) show lower ν_{as} (C–X–C) frequencies than the chloronium analogs (X = Cl), which is in line with the above assumption. In contrast, the trifluoromethylated derivatives (R = CF₃), which disfavors an ionic structure, show similar ν_{as} (C–X–C) frequencies for X = F and Cl (Supplementary Table 4).

Bonding analysis. Previous quantum-chemical studies focused on the atomic or partial charge of the fluorine atom in order to contest its classification as a fluoronium ion²⁸. Atomic charges, however, strongly depend on the computational level and are not uniquely defined²⁹. In the present case, a non-exhaustive selection of population analyses yields atomic charges for the bridging fluorine atom of –0.260 (NBO; all charges are given in atomic units), –0.136 (Mulliken), –0.132 (CHELPG), –0.521 (AIM), –0.094 (Merz–Kollmann), +0.058 (Voronoi) (for more details see Supplementary Table 6). For all methods, the neighboring carbon atoms yield a positive partial charge.

Perhaps a more relevant aspect is how the fluorine atom is bound to its two neighboring sp³-carbon atoms. As pointed out elsewhere, an AIM analysis shows two bond critical points (BCPs), indicating a chemical bond^{16,17}. Judging from the different properties at these BCPs ($\rho_{BCP} = 0.95 \text{ \AA}^{-3}$; $\nabla^2\rho_{BCP} = -6.43 \text{ \AA}^{-5}$; $\text{ELF}_{BCP} = 0.43$; $|V|/G = 2.05$) the bonds are barely covalent due to the strong fluorine-specific repulsion between lone pairs of the fluorine atom and the C–F σ -bonds and are best described as charge shift bonds^{30,31}. This bond character differs significantly from the one in [H–F–H]⁺ ($\rho_{BCP} = 2.03 \text{ \AA}^{-3}$; $\nabla^2\rho_{BCP} = -68.44 \text{ \AA}^{-5}$; $\text{ELF}_{BCP} = 0.98$; $|V|/G = 16.44$), which is genuinely covalent³².

To compare cation **1** to its heavier analogs, the fluorine atom was replaced by other halogens. The positions of the halogen atoms, the two neighboring carbon atoms, and the two nearest hydrogen atoms were re-optimized, while all other atoms were kept fixed. Table 2 lists the most important properties of the BCPs in these four systems and in [H–F–H]⁺.

As the X–C bond distance increases the X–C bond becomes less polarized and the BCP approaches the mid-point of the X–C bond path. With increasing bond length, the electron density and its curvature at the BCP decreases, although the number of

electrons associated with this bond increases, which can be seen from raising ELF (electron localization function) values and delocalization indices DLI_{X–C}. The covalent character in the chlorine analog is slightly larger than in the fluoronium cation and decreases again for the bromonium and iodonium cation. Nevertheless, it never reaches values typical for genuine covalent bonds as in [H–F–H]⁺. In Fig. 4, ELF maps for the fluoronium and chloronium cations are shown for the C–X–C plane (X = F, Cl; left) and the one perpendicular to that containing the halogen lone pairs (right; bromonium and iodonium ELF maps in Supplementary Fig. 4). All four systems clearly indicate covalent interactions between carbon and the halogen atom, with the fluoronium cation resembling the least genuine covalent interaction and the chloronium cation the most. In the former, the valence electrons of the fluorine atom seem the least polarized, resembling almost the ELF map of an ion. This might be reinforced by the adjacent hydrogen atoms that draw electron density from the lone pair region in the C–F–C plane, which can be considered as a fluorine-specific interaction. For the other halonium cations, the valence shell is clearly separated into a maximum along the C–X bond path and two distinguished lone pairs.

In all, our results—loosely analogous to the reported norbornyl cation crystal structure in 2013³³—definitively verify the nearly symmetrical structure of a controversial and often regarded as “impossible” species.

Methods

General considerations. All preparative work was carried out using standard Schlenk techniques. Glassware was greased with Triboflon III. All solid materials were handled inside a glove box with an atmosphere of dry argon (O₂ < 0.5 ppm, H₂O < 0.5 ppm). SO₂ClF was stored over CaH₂ before use. Precursor **2**, SbF₅·SO₂ and CsSb₂F₁₁ were made as reported^{16,17,34,35}.

IR. Low-temperature IR spectra were recorded on a Nicolet iS50 with a diamond ATR attachment and a home-build contraption which was cooled by a stream of liquid nitrogen to –40 °C.

X-ray crystallography. All data were recorded on a Bruker D8 Venture diffractometer with a CMOS area detector using a MoK α radiation source. In a nitrogen atmosphere suitable single crystals were coated and picked in per-fluoroether oil at –80 °C and subsequently mounted on a 0.15 mm Micromount. The structure solution and refinement were performed in OLEX2³⁶ utilizing the ShelXT³⁷ structure solution program with intrinsic phasing and the ShelXL³⁸ refinement package using least-squares on weighted F² values for all reflections.

Table 2 Computed properties of the bonds to the halogen atom in different double-norbornyl type halonium ions: bond length (r_{X-C}); deviation of the BCP from the mid-point of the bond ($r_{BCP-X} - 1/2r_{X-C}$; for negative values, the BCP is closer to the halogen atom, for positive values, vice versa); electron density at the BCP (ρ_{BCP}); Laplacian at the BCP ($\nabla^2\rho_{BCP}$); ELF at the BCP (ELF_{BCP}); value of the ELF maximum along the bond path (ELF_{max}); ratio of the absolute potential and the kinetic energy density at the BCP ($|V|/G$); localization index of the valence electrons at the halogen atom ($valLI_X$); delocalization index of the bonds with the halogen atom (DLI_{X-C}); localization index of the valence electrons at the carbon or hydrogen atom bound to the halogen atom ($valLI_{C/H}$).

System	r_{X-C} [Å]	$r_{BCP-X} - 1/2r_{X-C}$ [Å]	ρ_{BCP} [Å ⁻³]	$\nabla^2\rho_{BCP}$ [Å ⁻⁵]	ELF_{BCP}	ELF_{max}	$ V /G$	$valLI_X$	DLI_{X-C}	$valLI_{C/H}$
Fluoronium	1.5871	0.20	0.946	-6.432	0.43	-	2.05	6.72	0.58	1.84
Chloronium	1.8852	0.17	0.964	-2.614	0.80	0.87	2.49	5.82	0.85	1.91
Bromonium	2.0236	0.16	0.849	-1.616	0.82	0.83	2.40	4.73	0.89	1.95
Iodonium	2.2006	0.14	0.729	-1.099	0.80	0.82	2.33	5.32	0.94	2.03
[H-F-H] ⁺	0.9679	0.35	2.027	-68.62	0.98	-	16.5	7.42	0.27	0.01

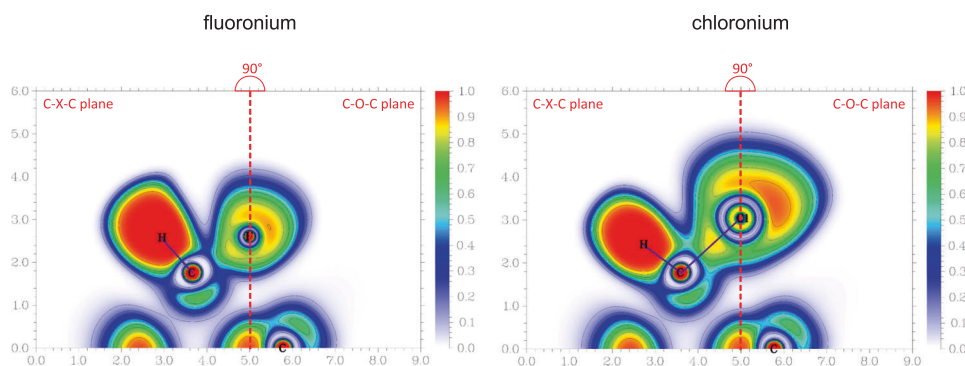


Fig. 4 Electron localization in Fluoro- and Chloronium. Electron localization function in the C-X-C plane (X = F, Cl) of 1 (left) and its chloronium analog (right) and in their C-O-C planes containing the halogen's lone pairs, perpendicular to the former one. Both planes are merged at the molecule's O-X axis (dashed red line). ELF is defined from 0.0 (white) to 1.0 (red); contours are drawn in intervals of 0.1.

Computational details. Calculations were performed with the Gaussian³⁹ program, using the B3LYP DFT functional applying Dunning's cc-pVTZ basis set⁴⁰⁻⁴² for all atoms except iodine for which a fully relativistic pseudopotential replacing 28 core electrons and the corresponding triple- ζ basis set^{43,44} was used. All population analyses, AIM analysis, as well as the calculation and visualization of ELF plots, were performed with the Multiwfn program⁴⁵. In addition, the Turbomole program⁴⁶ was used to perform calculations at the unrestricted Kohn-Sham DFT level, using the B3LYP hybrid functional⁴⁷⁻⁴⁹ in conjunction with the valence triple- ζ basis set with two sets of polarization functions (def2-TZVPP)⁵⁰.

Crystallization of fluoronium salt [1][Sb₂F₁₁]. After SbF₅·SO₂ (26 mg, 0.093 mmol) was filled into a Schlenk tube, SO₂ClF was condensed into the vessel forming a clear solution at -50 °C. Precursor 2 (20 mg, 0.075 mmol) was added via a funnel to the reaction vessel and the mixture was shaken until a homogenous yellow solution was formed. After the partial evacuation of the solvent, the mixture was slowly cooled to -80 °C. Over the course of two weeks, yellow crystals started to grow which could be analyzed via X-ray diffraction.

Pumping off all volatiles from the crystalline material under reduced pressure produced an orange powder, of which a sample for low-temperature IR measurements was prepared.

IR (ATR, -40 °C): $\tilde{\nu}$ = 2990 (w, ν (C-H)), 2914 (w, ν (C-H)), 1913 (m, ν (C=O)), 1746 (w), 1614 (s, ν_{as} (C=O...Sb)), 1562 (m), 1492 (w), 1475 (w), 1443 (m), 1394 (w), 1359 (m), 1327 (w), 1304 (m), 1292 (w), 1275 (w), 1258 (w), 1218 (m), 1172 (m), 1136 (w), 1100 (m), 1068 (w), 1056 (w), 1042 (w), 1025 (w), 988 (w), 918 (w), 870 (w), 822 (m, ν_{as} (C-O-C)), 793 (w), 736 (w), 701 (sh, ν_s (C-F-C)), 685 (vs, ν (Sb-F)), 669 (vs, ν (Sb-F)), 640 (s, ν (Sb-F)), 629 (s, ν (Sb-F)), 581 (s, ν_{as} (C-F-C)), 551 (m), 516 (m, δ (C-F-C)), 502 (m), 476 (m, ν (Sb-F-Sb)), 430 (w), 417 (w), 408 (w), 384 (w), 364 (w), 272 (sh, ρ (C-F-C)), 237 (vs, δ (Sb-F-Sb)), 181 (w), 172 (w) cm⁻¹. (vs = very strong, s = strong, m = medium, w = weak, sh = shoulder).

Data availability

Crystallographic data (excluding structure factors) for structures reported in this study have been deposited at the Cambridge Crystallographic Data Centre (CCDC) and can be

obtained free of charge via www.ccdc.cam.ac.uk/data_request/cif on quoting the depository number CCDC-2049161. All other data generated or analyzed during this study are provided in this Article and the Supplementary Information.

Received: 29 March 2021; Accepted: 11 August 2021;

Published online: 06 September 2021

References

- McNaught, A. D. & Wilkinson, A. *IUPAC. Compendium of Chemical Terminology (the "Gold Book")* 2nd edn (Blackwell Scientific Publications, Oxford, 1997).
- Roberts, I. & Kimball, G. E. The halogenation of ethylenes. *J. Am. Chem. Soc.* **59**, 947-948 (1937).
- Grushin, V. V. Cyclic diaryliodonium ions: old mysteries solved and new applications envisaged. *Chem. Soc. Rev.* **29**, 315-324 (2000).
- Bailey, F., Barthen, P., Frohn, H.-J. & Köckerling, M. Aryl(pentafluorophenyl) iodonium tetrafluoroborate: Allgemeine Synthesemethode, typische Eigenschaften und strukturelle Gemeinsamkeiten. *Z. Anorg. Allg. Chem.* **626**, 2419-2427 (2000).
- Brown, R. S. et al. Stable bromonium and iodonium ions of the hindered olefins adamantylideneadamantane and bicyclo[3.3.1]nonylidenebicyclo[3.3.1]nonane. X-ray structure, transfer of positive halogens to acceptor olefins, and ab initio studies. *J. Am. Chem. Soc.* **116**, 2448-2456 (1994).
- Frohn, H.-J., Giesen, M., Welting, D. & Bardin, V. V. Bis(perfluoroorganyl) bromonium salts [(RF)₂Br]⁺Y⁻ (RF=aryl, alkenyl, and alkynyl). *J. Fluor. Chem.* **131**, 922-932 (2010).
- Stoyanov, E. S., Stoyanova, I. V., Tham, F. S. & Reed, C. A. Dialkyl chloronium ions. *J. Am. Chem. Soc.* **132**, 4062-4063 (2010).
- Hämmerling, S. et al. A very strong methylation agent: [Me₂Cl][Al(OTeF₅)₄]. *Angew. Chem. Int. Ed.* **58**, 9807-9810 (2019).
- Hämmerling, S. et al. Ein sehr starkes Methylierungsmittel: [Me₂Cl][Al(OTeF₅)₄]. *Angew. Chem.* **131**, 9912-9915 (2019).

- Olah, G. A., Laali, K. K., Wang, Q. & Prakash, G. K. S. *Onium Ions* (Wiley, New York, NY, 1998).
- Olah, G. A. *Halonium Ions* (Wiley, New York, NY, 1975).
- Viet, N., Cheng, X. & Morton, T. H. Three-membered cyclic fluoronium ions in gaseous ion-neutral complexes. *J. Am. Chem. Soc.* **114**, 7127–7132 (1992).
- Wang, H., Webster, C. E., Pérez, L. M., Hall, M. B. & Gabbai, F. P. Reaction of the 1,8-bis(diphenylmethyl)napthalenediyl dication with fluoride: formation of a cation containing a C-F→C bridge. *J. Am. Chem. Soc.* **126**, 8189–8196 (2004).
- Struble, M. D., Scerba, M. T., Siegler, M. & Lectka, T. Evidence for a symmetrical fluoronium ion in solution. *Science* **340**, 57–60 (2013).
- Struble, M. D., Holl, M. G., Scerba, M. T., Siegler, M. A. & Lectka, T. Search for a symmetrical C-F-C fluoronium ion in solution: kinetic isotope effects, synthetic labeling, and computational, solvent, and rate studies. *J. Am. Chem. Soc.* **137**, 11476–11490 (2015).
- Pitts, C. R., Holl, M. G. & Lectka, T. Spectroscopic characterization of a [C-F-C]⁺ fluoronium ion in solution. *Angew. Chem. Int. Ed.* **57**, 1924–1927 (2018).
- Pitts, C. R., Holl, M. G. & Lectka, T. Spectroscopic characterization of a [C-F-C]⁺ fluoronium ion in solution. *Angew. Chem.* **130**, 1942–1945 (2018).
- Mootz, D. & Bartmann, K. The fluoronium ions H₂F⁺ and H₃F₂⁺: characterization by crystal structure analysis. *Angew. Chem. Int. Ed. Engl.* **27**, 391–392 (1988).
- Panisch, R., Bolte, M. & Müller, T. Hydrogen- and fluorine-bridged disilyl cations and their use in catalytic C-F activation. *J. Am. Chem. Soc.* **128**, 9676–9682 (2006).
- Lehmann, M., Schulz, A. & Villinger, A. Bisilylated halonium ions: [Me₃Si-X-SiMe₃][B(C₆F₅)₄] (X=F, Cl, Br, I). *Angew. Chem. Int. Ed.* **48**, 7444–7447 (2009).
- Lehmann, M., Schulz, A. & Villinger, A. Bisilylated halonium ions: [Me₃Si-X-SiMe₃][B(C₆F₅)₄] (X=F, Cl, Br, I). *Angew. Chem.* **121**, 7580 (2009).
- Ivlev, S. I., Karttunen, A. J., Buchner, M. R., Conrad, M. & Kraus, F. The interhalogen cations [Br₂F₃]⁺ and [Br₃F₈]⁺. *Angew. Chem. Int. Ed.* **57**, 14640–14644 (2018).
- Ivlev, S. I., Karttunen, A. J., Buchner, M. R., Conrad, M. & Kraus, F. Die Interhalogenkationen [Br₂F₃]⁺ und [Br₃F₈]⁺. *Angew. Chem.* **130**, 14850–14855 (2018).
- Nakamoto, K. *Infrared and Raman Spectra of Inorganic and Coordination Compounds A: Theory and Applications in Inorganic Chemistry* (John Wiley & Sons Inc, Hoboken, N.J., 2009).
- Solcà, N. & Dopfer, O. Protonation of gas-phase aromatic molecules: IR spectrum of the fluoronium isomer of protonated fluorobenzene. *J. Am. Chem. Soc.* **125**, 1421–1430 (2003).
- Minkwitz, R. & Gerhard, V. On dimethylhalonium salts - CH₃ClCH₃⁺MF₆⁻, CH₃BrCH₃⁺MF₆⁻, CH₃ICH₃⁺MF₆⁻ and dimethylmethylendiiodonium salts (CH₃ICH₂ICH₃)₂⁺(MF₆⁻)₂ (M = As, Sb). *Z. Naturforsch. B Chem. Sci.* **46**, 561–565 (1991).
- Stoyanov, E. S. Chemical properties of dialkyl halonium ions (R₂Hal⁺) and their neutral analogues, methyl carboranes, CH₃-(CHB₁₁Hal₁₁), where Hal = F, Cl. *J. Phys. Chem. A* **121**, 2918–2923 (2017).
- Christe, K. O., Haiges, R., Rahm, M., Dixon, D. A. & Vasiliu, M. Misconceptions on fluoronium ions and hypervalent fluorine cations. *J. Fluor. Chem.* **204**, 6–10 (2017).
- Mao, J. X. Atomic charges in molecules: a classical concept in modern computational chemistry. *PDJ* **2**, 15–18 (2014).
- Shaik, S. et al. Charge-shift bonding: a new and unique form of bonding. *Angew. Chem. Int. Ed.* **59**, 984–1001 (2020). *Angew. Chem.* **132**, 996–1013 (2020).
- Shaik, S. et al. Charge-shift bonding: a new and unique form of bonding. *Angew. Chem.* **132**, 996–1013 (2020).
- Espinosa, E., Alkorta, I., Elguero, J. & Molins, E. From weak to strong interactions: a comprehensive analysis of the topological and energetic properties of the electron density distribution involving X-H...F-Y systems. *J. Chem. Phys.* **117**, 5529–5542 (2002).
- Scholz, F. et al. Crystal structure determination of the nonclassical 2-norbornyl cation. *Science* **341**, 62–64 (2013).
- Aynsley, E. E., Peacock, R. D. & Robinson, P. L. New inorganic compounds involving antimony pentafluoride. *Chem. Ind.* 1117 (1951).
- Benkič, P., Brooke Jenkins, H. D., Ponikvar, M. & Mazej, Z. Synthesis and characterisation of alkali metal and thallium polyfluoroantimonates, ASb_nF_{5n+1} (n = 2, 3). *Eur. J. Inorg. Chem.* **2006**, 1084–1092 (2006).
- Dolomanov, O. V., Bourhis, L. J., Gildea, R. J., Howard, J. A. K. & Puschmann, H. OLEX 2: a complete structure solution, refinement and analysis program. *J. Appl. Cryst.* **42**, 339–341 (2009).
- Sheldrick, G. M. A short history of SHELX. *Acta Crystallogr. A* **64**, 112–122 (2008).
- Sheldrick, G. M. Crystal structure refinement with SHELXL. *Acta Cryst. C* **71**, 3–8 (2015).
- Frisch, M. J. et al. *Gaussian 16* (Gaussian, Inc., Wallingford CT, 2016).
- Dunning, T. H. Gaussian basis sets for use in correlated molecular calculations. I. The atoms boron through neon and hydrogen. *J. Chem. Phys.* **90**, 1007–1023 (1989).
- Woon, D. E. & Dunning, T. H. Gaussian basis sets for use in correlated molecular calculations. III. The atoms aluminum through argon. *J. Chem. Phys.* **98**, 1358–1371 (1993).
- Wilson, A. K., Woon, D. E., Peterson, K. A. & Dunning, T. H. Gaussian basis sets for use in correlated molecular calculations. IX. The atoms gallium through krypton. *J. Chem. Phys.* **110**, 7667–7676 (1999).
- Peterson, K. A., Figgen, D., Goll, E., Stoll, H. & Dolg, M. Systematically convergent basis sets with relativistic pseudopotentials. II. Small-core pseudopotentials and correlation consistent basis sets for the post-d group 16–18 elements. *J. Chem. Phys.* **119**, 11113–11123 (2003).
- Peterson, K. A., Shepler, B. C., Figgen, D. & Stoll, H. On the spectroscopic and thermochemical properties of ClO, BrO, IO, and their anions. *J. Phys. Chem. A* **110**, 13877–13883 (2006).
- Lu, T. & Chen, F. Multiwfn: a multifunctional wavefunction analyzer. *J. Comput. Chem.* **33**, 580–592 (2012).
- TURBOMOLE GmbH. *TURBOMOLE V7.3* (a development of University of Karlsruhe and Forschungszentrum Karlsruhe GmbH, 1989–2018).
- Becke, A. D. Density-functional exchange-energy approximation with correct asymptotic behavior. *Phys. Rev. A* **38**, 3098–3100 (1988).
- Lee, C., Yang, W. & Parr, R. G. Development of the Colle-Salvetti correlation-energy formula into a functional of the electron density. *Phys. Rev. B* **37**, 785–789 (1988).
- Vosko, S. H., Wilk, L. & Nusair, M. Accurate spin-dependent electron liquid correlation energies for local spin density calculations: a critical analysis. *Can. J. Phys.* **58**, 1200–1211 (1980).
- Weigend, F. & Ahlrichs, R. Balanced basis sets of split valence, triple zeta valence and quadruple zeta valence quality for H to Rn: design and assessment of accuracy. *Phys. Chem. Chem. Phys.* **7**, 3297–3305 (2005).

Acknowledgements

We thank J. Heberle and D. Ehrenberg for scientific discussions. We gratefully acknowledge the Zentraleinrichtung für Datenverarbeitung (ZEDAT) of the Freie Universität Berlin for the allocation of computer time. Funded by the Deutsche Forschungsgemeinschaft (DFG, German Research Foundation)—Project-ID 387284271—SFB 1349. M.K. thanks JHU for a William Hooper Grafflin Fellowship (M.K.) and the National Science Foundation (NSF) (Grant CHE 1800510) (T.L.) for financial assistance.

Author contributions

K.F.H. carried out the synthetic work and analytical characterization. A.W. performed preliminary experiments on the system. C.M. and K.F.H. performed DFT calculations. C.M. performed the bonding analysis. S.S. acquired the XRD data. H.B. assisted with vibrational data analysis. M.K. and C.R.P. synthesized precursor 2. K.F.H. wrote the paper, all authors discussed and commented on the manuscript. T.L. and S.R. directed and coordinated the research.

Funding

Open Access funding enabled and organized by Projekt DEAL.

Competing interests

The authors declare no competing interests.

Additional information

Supplementary information The online version contains supplementary material available at <https://doi.org/10.1038/s41467-021-25592-6>.

Correspondence and requests for materials should be addressed to T.L. or S.R.

Peer review information *Nature Communications* thanks Karl Christe and the anonymous reviewer(s) for their contribution to the peer review of this work.

Reprints and permission information is available at <http://www.nature.com/reprints>

Publisher's note Springer Nature remains neutral with regard to jurisdictional claims in published maps and institutional affiliations.



Open Access This article is licensed under a Creative Commons Attribution 4.0 International License, which permits use, sharing, adaptation, distribution and reproduction in any medium or format, as long as you give appropriate credit to the original author(s) and the source, provide a link to the Creative Commons license, and indicate if changes were made. The images or other third party material in this article are included in the article's Creative Commons license, unless indicated otherwise in a credit line to the material. If material is not included in the article's Creative Commons license and your intended use is not permitted by statutory regulation or exceeds the permitted use, you will need to obtain permission directly from the copyright holder. To view a copy of this license, visit <http://creativecommons.org/licenses/by/4.0/>.

© The Author(s) 2021